

Single-step preparation of fluorescent carbon nanoparticles, and their application as a fluorometric probe for quercetin

Pengli Zuo · Deli Xiao · Mengmeng Gao · Jun Peng · Renfeng Pan · Yang Xia · Hua He

Received: 14 December 2013 / Accepted: 13 March 2014 / Published online: 23 April 2014
© Springer-Verlag Wien 2014

Abstract We report on a method for the determination of quercetin based on the quenching of the fluorescence of carbon nanoparticles (CNPs). The CNPs were prepared by carefully adding an aqueous solution of glucose to solid diphosphorus pentoxide. This single-step method proceeds rapidly and gives large quantities of CNPs. Neither high temperatures nor complicated synthesis steps are needed. The resulting CNPs have an average size of 120 nm and were characterized by high-resolution TEM, FT-IR, elemental analysis and spectrofluorometry. The fluorescence of the CNPs decreases with increasing concentrations of the flavonoid quercetin, with a linear response to quercetin in the 3.3 to 41.2 μM concentration range in pH 6.0 water solution and also in a solution containing 16 % (v/v) of fetal bovine serum. The detection limit is as low as 0.175 μM , and the Stern-Volmer quenching constant is $4.34 \times 10^4 \text{ M}^{-1}$.

Keywords Fluorescent carbon nanoparticles · Quercetin · Fluorescence quenching · Fetal bovine serum

Pengli Zuo and Deli Xiao these authors contributed equally to this work.

Electronic supplementary material The online version of this article (doi:10.1007/s00604-014-1236-3) contains supplementary material, which is available to authorized users.

P. Zuo · D. Xiao · M. Gao · J. Peng · R. Pan · H. He (✉)
Department of Analytical Chemistry, China Pharmaceutical University, Nanjing 210009, China
e-mail: dochehua@163.com

Y. Xia (✉)
Department of Rehabilitation Medicine, Zhongda Hospital Southeast University, Nanjing 210009, China
e-mail: xiayang918@126.com

H. He
Key Laboratory of Drug Quality Control and Pharmacovigilance, Ministry of Education, China Pharmaceutical University, Nanjing 210009, China
e-mail: jcb315@163.com

Introduction

Quercetin is a typical polyhydroxy flavonoid compound, which is found abundantly in flowers, leaves, barks and fruits of many kinds of plants. Quercetin is not only found in medicinal botanicals, including Ginkgo biloba, Hypericum perforatum (St. John's wort), and Sambucus canadensis (elder) [1, 2], but also found in a variety of foods including apples, berries, capers, grapes, onions, tea and tomatoes, as well as many nuts. During the past years, quercetin has gained tremendous interest because it has many potential beneficial effects on human health including cardiovascular protection, anticancer activity, antiulcer effects, anti-allergy activity, antibacterial, antiviral activity and anti-inflammatory effects [3]. Most of these beneficial effects were known due to the antioxidant activity of quercetin [4], because quercetin is an excellent free-radical scavenging antioxidant, which benefits from its high number of hydroxyl groups and conjugated π orbitals. By these functional groups, quercetin could donate electrons or hydrogen, and scavenge H_2O_2 and superoxide anion ($\bullet\text{O}_2^-$) [5]. Thus it is of significance to develop an appropriate approach to detect quercetin in biological samples, pharmaceutical samples and in natural products. So far, various analytical methods have been employed for the determination of quercetin, such as high-performance liquid chromatography [6], capillary electrophoresis [7] and electroanalytical methods [8]. Several fluorescence methods [9, 10] have also been reported. These techniques may provide high selectivity, but have some disadvantages such as operating complexity, time and cost consumption.

Quantum dots are a kind of quasi-zero-dimensional nanomaterials, they show very good fluorescence stability, wide excitation and emission spectra, which enabling them to be exploited in many potential applications. However, conventional quantum dots are usually

made from semiconducting materials, especially cadmium and selenium, in organic-phase or in water-phase system, which has raised concerns over toxicity and high cost. As a result, more benign fluorescent carbon nanoparticles (CNPs) have gained increasing research attention in the past decade, because of their super solubility in water, excellent optical property, chemical inertness, low cytotoxicity, easy functionalization and resistance to photobleaching [11]. Highly fluorescent carbon nanoparticles can be synthesized inexpensively through lots of one-step approaches on a large scale, these approaches include simple chemical oxidation reaction [12, 13], electrochemical method [14], ultrasonic treatment, microwave method [15], template method [16] and laser ablation strategy [17], etc. Microwave-assisted method [18, 19] and hydrothermal treatment [20] have been widely used. Xiao et al. [19] used a domestic microwave oven (700 W) and heated for different time periods to prepare CNPs, the reaction temperature was hard to control, so explosion often took place, the reaction gave off thick smog, and the smell was very strong. Recently, the fluorescent carbon nanoparticles (CNPs) have been the most promising emerging fluorescent labels for cellular imaging, photocatalysis, energy conversion/storage, bioimaging, optoelectronics, optical limiting sensors [11]. Because of CNPs's fluorescence (FL) properties, they have also been used for different analytical applications. Lu et al. [20] used fluorescent carbon nanoparticles as probes for sensitive and selective detection of mercury ions. CNPs also could be used as probes to detect copper ions [21]. Li et al. [22] used CNPs as an effective fluorescent sensing platform for nucleic acid detection. Fang et al. [23] synthesized fluorescent carbon nanoparticles based on chemical oxidation reaction using acetic acid acted as the oxygenous carbon resource. This was an automatic method without heat to rapidly produce large quantities of carbon nanoparticles (CNPs), but the monodispersity of CNPs was poor, what's more, many other carbon precursors were not investigated.

Therefore, to begin with, we prepared novel water-soluble CNPs by an automatic method using glucose which is cheap and easy to get as carbon source, this automatic method was eco-friendly and safely. Besides, CNPs could serve as an effective fluorescent probe for label-free, sensitive, and selective detection of quercetin. Moreover, the effect of concentration of CNPs, buffer solutions, ionic strength, pH and potentially interfering substances on the fluorescence intensity of CNPs for the determination of quercetin was investigated. Eventually, the calibration and detection limit of the method were studied. To demonstrate the practicality of this fluorescence probe, it was applied to the determination of

quercetin in fetal bovine serum solution, which was more complicated than buffer solution.

Experimental

Apparatus

UV-vis absorption was characterized by a UV1800 UV-vis spectrophotometer (Shimadzu Corporation, Japan). Photoluminescence (PL) emission measurements were performed using a RF-5301PC fluorescence spectrophotometer (Shimadzu Corporation, Japan). The morphology of the synthesized nanoparticles was studied using a JEM-2100(HR) transmission electron microscope (TEM) (JEOL, Japan). The sample for TEM characterization was prepared by placing a drop of colloidal solution on carbon-coated copper grid and dried at room temperature. FT-IR spectrum was performed on a Shimadzu IR-prespige-21 FT-IR spectrometer (Kyoto, Japan) in the range of 400–4,000 cm^{-1} . Result of element analyzing was acquired with an Elementar Vario ELIII. Zeta potential was analyzed using ZetaPALS Zeta Potential/Particle Sizer (Brookhaven, USA).

Materials and reagents

Glucose was purchased from Nanjing Chemical Reagent Co., Ltd. (Nanjing, China; <http://www.nj-reagent.com>), Quercetin was purchased from Sinopharm Chemical Reagent Co., Ltd. (Shanghai, China; www.reagent.com.cn). Fetal bovine serum was purchased from Shanghai Boyao Bio-Tech Co., Ltd (Shanghai, China; www.shbybio.net). All the chemicals were used without any further purification. Doubly deionized water was used throughout.

Preparation of fluorescent CNPs

Fluorescent CNPs were synthesized as follows: Glucose (0.5 g) was mixed with 2 mL of deionized water under ultrasound for 10 min to form a homogeneous solution, which was then added to 2.5 g of P_2O_5 in a 25 mL beaker without stirring. The reaction mixture was quickly foamed by the spontaneous heat, and then gradually cooled to room temperature. The CNPs in the dark brown mixture were dispersed in water, centrifuged at 13,000 rpm for 30 min to collect the supernatant, then dialyzed against pure water through a dialysis membrane for 1 day to remove residual glucose and ions. Finally, fluorescent CNPs were concentrated to 0.5 mL in vacuum at 65 °C overnight. Following the same process, we prepared several batches of CNPs.

Quantum yield measurements

The quantum yield (Φ) of CNPs was calculated according to:

$$\Phi = \Phi_R \times \frac{I}{I_R} \times \frac{A_R}{A} \times \frac{\eta^2}{\eta_R^2}$$

Where Φ is the quantum yield, I is the measured integrated emission peak area, η is the refractive index and A is the UV absorbance at 370 nm. The subscript R refers to the reference quinine sulfate. Quinine sulfate (QS) (literature $\Phi_R=0.54$) used as a standard was dissolved in 0.1 M H_2SO_4 ($\eta=1.33$) and the CNPs were dissolved in distilled water ($\eta=1.33$). The absorbance of CNPs and quinine sulfate solution were adjusted never exceed 0.05 at excitation wavelength 370 nm.

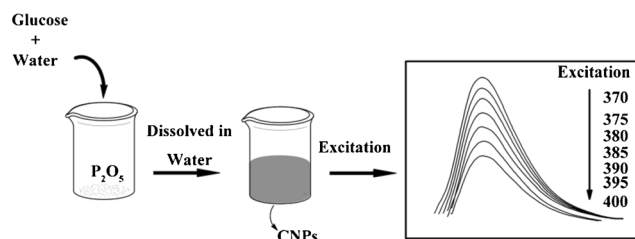
Determination of quercetin in fetal bovine serum solution

In a 5 mL volumetric flask was successively placed 330 μL of CNPs, 0.8 mL fetal bovine serum and an appropriate volume of quercetin solution. The mixture was then diluted to the mark with phosphate buffer solution (0.01 mol L^{-1} , pH 6.0) and mixed thoroughly. The fluorescent emission spectra were obtained by scanning the emission from 300 to 700 nm on the spectrofluorimeter after reaction for 22 min at room temperature (with 5 and 5 nm slit width for excitation and emission, respectively). F and F_0 , which are the FL intensity of the CNPs in the presence and absence of quercetin respectively, were measured at 370 nm in fetal bovine serum solution. The sensitivity and selectivity measurements were conducted in triplicate.

Results and discussion

Preparation of CNPs

As shown in Scheme 1, fluorescent CNPs were synthesized as follows: an appropriate amount of glucose was dissolved in water to form a homogeneous solution, which was added to 2.5 g of P_2O_5 in a 25 mL beaker without stirring. Glucose acted as the oxygenous carbon resource, which induced oxygenous defects [24]. Water quickly reacted with P_2O_5 , and continuous heat was produced. P_2O_5 turned into phosphoric acid and polyphosphoric acid (PPA) [25]. Due to the catalysis by both PPA and P_2O_5 , the carbonization reaction started and continued at 100 $^\circ\text{C}$. In this system, the upper temperature was mainly controlled by vaporizing water at its boiling point. The color of the mixture changed to brown within 20 s, and the volume of the sticky slurry mixture was dramatically expanded by foaming because of the boiling of water by the spontaneous heat. The reaction lasted for about 10 min until the exhaustion of P_2O_5 . The obtained dark brown



Scheme 1 A schematic illustration of preparation procedure of CNPs by carbonization of glucose

mixture was centrifuged and dialyzed to remove ions and residual glucose. Finally, a clear yellow–brown aqueous solution containing CNPs was obtained. All the prepared fluorescent CNPs of several batches showed good water solubility and there was no precipitation for months. Our preparation method presented a facile approach to produce high fluorescent CNPs on a large scale.

Characterization of CNPs

In a 5 mL volumetric flask was successively placed 330 μL of CNPs, it was then diluted to the mark with phosphate buffer solution (0.01 mol L^{-1} , pH 6.0) and mixed thoroughly. The fluorescent emission spectra were obtained by scanning the emission from 300 to 700 nm on the spectrofluorimeter at room temperature (with 5 and 5 nm slit width for excitation and emission, respectively). Figure 1 depicts the UV–vis absorption and PL spectra for CNPs. The maximum UV absorption peak was observed at 281.5 nm, which may be attributed to $n\text{-}\pi^*$ transitions of $\text{C}=\text{O}$ [26]. When CNPs were excited at 370 nm, the PL spectra showed a peak position at 438 nm, which was relatively narrow and symmetric. In addition, the fluorescent intensity gradually decreased with increasing excitation wavelength from 370 to 390 nm, which may be attributed to the different emissive traps on the CNPs surface. The fluorescence intensity excited at 370 nm was the highest and used for quantitative analysis afterward. Interestingly, the emission spectra of the CNPs had no shift as the excitation wavelength changed, which was quite different from many previous reports [11]. This phenomenon might

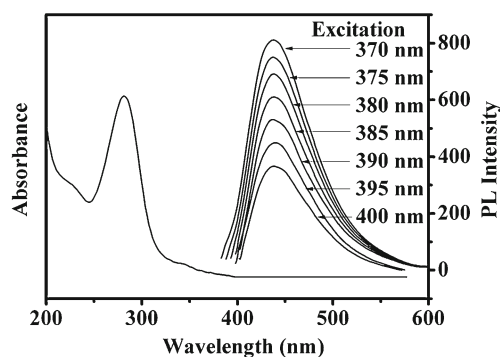


Fig. 1 UV–vis absorption spectra and Photoluminescence spectra for CNPs; concentration of CNPs, 66 $\mu\text{L mL}^{-1}$ (V/V)

be caused by fluorescence resonance energy transfer [21]. Förster resonant energy transfer (FRET), one kind of fluorescence resonance energy transfer, is a nonradiative energy transfer mechanism between an excited donor and an acceptor through dipole-dipole interactions. There were many bubbles in the CNPs, as we could see in Fig. 2c. Most bubbles were in the size of 1–10 nm, which was in the distance limit of FRET. The CNPs were divided into many parts, some acted as donors, while others served as acceptors. They were in close proximity to each other to constitute FRET systems in one CNP [27]. This donor-acceptor system leads to intra-energy transfer [28], so that there were no wavelength shifts when excited with light of different wavelengths.

The fluorescence quantum yield of CNPs was 0.0799 at the excitation of 370 nm with quinine sulfate as a standard reference, and these values were comparable with previous reports [29, 30]. The reason that the synthesized particles showed a good quantum yield in spite of their big size was that the synthesized big particles were made up of many little particles which formed rigid structure (Fig. 2c), this rigid structure could reduce the collision among the little particles and the energy loss.

The TEM image (Fig. 2) shows that the CNPs were dispersed with spherical shape. The size of most prepared nanoparticles was about 120 nm in diameter. In the process of automatic synthesis, the mixture was greatly foamy because of the boiling of water, the carbon nanoparticles were linked with each other to form larger hollow nanoparticles (Fig. 2c). Table S1 (Electronic Supplementary Material, ESM) shows comparison of the properties of CNPs prepared by different synthetic methods, suggesting the properties of CNPs vary greatly from method to method. Elemental analysis indicated that the composition of the CNPs was: C 48.9 wt.%, H 4.84 wt.% and O 46.26 wt.%; The composition of glucose was: C 36.35 wt.%, H 6.99 wt.% and O 56.66 wt.%. It was

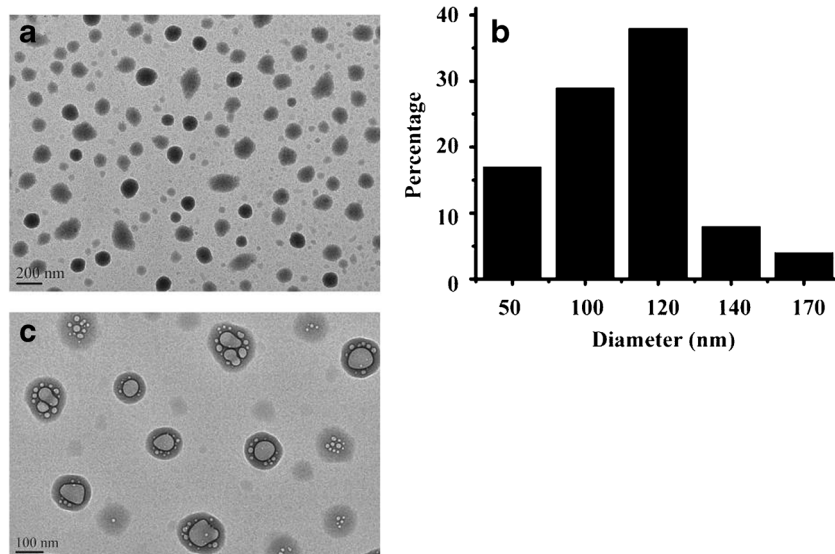
found that after carbonization reaction the carbon content of the CNPs increased, while the oxygen content of the CNPs decreased greatly.

As shown in Fig. 3, Fourier transform infrared (FT-IR) measurements of pure glucose powder showed that the peak at $3,369\text{ cm}^{-1}$ was attributed to O-H stretching vibration. The peak at $1,636\text{ cm}^{-1}$ corresponded to C = O stretching vibration. The peak at $1,047\text{ cm}^{-1}$ was attributed to C-O stretching vibrations. For the CNPs, the result showed large increase in absorption of O-H stretching vibrations at $3,369\text{ cm}^{-1}$, C = O stretching vibration at $1,636\text{ cm}^{-1}$ and C-O stretching vibrations at $1,006\text{ cm}^{-1}$ compared with glucose, furthermore, the zeta potential of the CNPs in water was measured to be -11.2 mV . These data revealed that the obtained CNPs had a lot of carboxylic groups on their surface. These distinctions may be caused by the degradation of glucose and the formation of crosslinked carbon nanodomains through carbonization reaction. Similar results were also reported in the literature [21].

Effect of quercetin concentration on the fluorescence intensity of CNPs

Figure 4 illustrates the emission spectra of CNPs in fetal bovine serum solution and their fluorescence titration with quercetin. The results indicated that the fluorescence intensity of CNPs at 438 nm (excitation 370 nm) decreased significantly with the increase of quercetin concentrations, but there was no emission spectra maximum shift (Fig. 4). In order to develop a sensitive fluorescence method for detection of quercetin in aqueous solution, which is based on quercetin induced fluorescence quenching of CNPs, several parameters such as pH, ionic strength, and reaction time were evaluated.

Fig. 2 TEM images and their size distributions for CNPs; scale bars: 200 nm (a), 100 nm (c), the corresponding particle size distribution histogram (b)



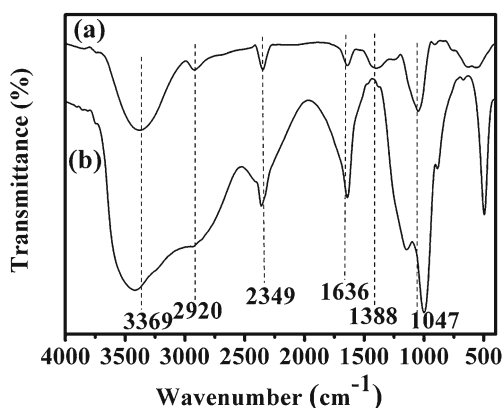


Fig. 3 FT-IR spectrum of glucose (a) and CNPs (b)

Effect of pH

The influence of various buffers on the fluorescence intensity of the system was investigated by using Tris-HCl, citric acid-sodium citrate, phosphate and $\text{NH}_3\text{-NH}_4\text{Cl}$ buffers at various pH values. Under the same conditions, the fluorescence intensity of the CNPs was the highest in phosphate buffer among the 4 buffers used, a satisfactory result for the detection of quercetin was obtained in phosphate buffers.

The impact of different buffer pH values on the fluorescence intensity of CNPs was also investigated. The results showed that varying buffer pH values could lead to a drastic change of fluorescence intensity of CNPs, which could influence the sensitivity and selectivity towards target materials. In order to develop a sensitive spectrophotometric method for determination of quercetin in a fetal bovine serum solution, the effect of pH values between 4.3 and 9.2 of the solution on the fluorescence intensity was studied to select the optimum conditions for the determination and the results were shown in Fig. 5. Since the fluorescence intensity in phosphate buffer

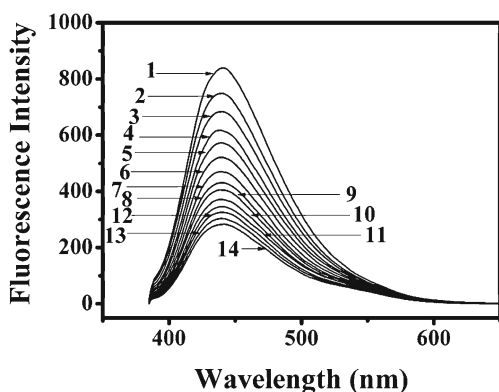


Fig. 4 Fluorescence emission spectra of CNPs in the absence and presence of different concentrations of quercetin in fetal bovine serum solution; $\lambda_{\text{ex}}=370$ nm; concentration of CNPs, $66 \mu\text{L mL}^{-1}$ (V/V), concentration of fetal bovine serum, $160 \mu\text{L mL}^{-1}$ (V/V), quercetin from (1) to (14): 0, 3.30, 6.58, 9.83, 13.07, 16.28, 19.45, 22.63, 25.78, 28.92, 32.03, 35.11, 38.18 and $41.23 \times 10^{-6} \text{ mol L}^{-1}$

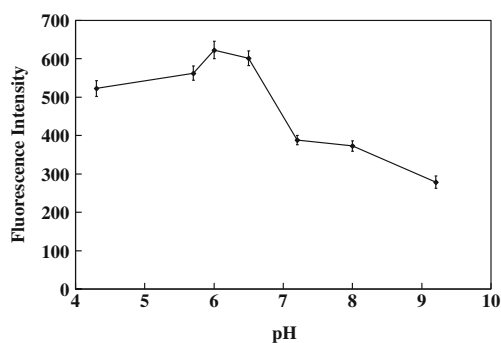


Fig. 5 The effect of solution pH value on CNPs fluorescence. The error bars represent standard deviations based on three independent measurements at each pH

solution was the highest at pH 6.0, the optimal pH was chosen to be 6.0, near the pH value of most neutral samples.

Effect of ionic strength

The effect of different concentrations of phosphate buffer solution was investigated. It exhibited that the fluorescence intensity of the complex decreased significantly with the increase of phosphate buffer solution concentration from 0.01 to 0.20 mol L^{-1} at pH 6.0. Since the intensity at 0.01 mol L^{-1} was the highest and remained stable, the optimal concentration of phosphate buffer solution was chosen as 0.01 mol L^{-1} .

Effect of reaction time

At room temperature, experiments demonstrated that the fluorescence intensity of CNPs in the absence and presence of different concentrations of quercetin changed slightly and tended to be stable after 22 min. Therefore, only 22 min was required to complete the reaction between CNPs and quercetin. We recorded the fluorescence intensity after the system had reacted for 22 min at room temperature. This system exhibited rapid reaction rate and good stability.

Study of potentially interfering substances

Many compounds and metal ions have the potential to quench CNPs fluorescence emissions [31, 32]. In order to assess the selectivity of the method, the influence of familiar potentially interfering substances were tested. As seen in Table S2 (ESM), this method was free from the interference of some metal ions, glucose, urea and amino acid as well as ascorbic acid, but other flavonoids such as luteolin and kaempferol could change fluorescence intensity significantly, because their chemical structures are very close to that of quercetin.

Table 1 Figures of merits of comparable methods for determination of quercetin

Methods	Linear range	LOD	Comments	Reference
Voltammetric determination	1.0×10^{-7} -1.0×10^{-6} M	3.0×10^{-8} M	Specific detection of quercetin; Detection in aqueous solution, in the diluted blood serms and urine	[35]
CE-ED	0.5×10^{-6} -1.0×10^{-3} M	2.25×10^{-7} M	Expensive, time-consuming, Insensitive; Detection in organic solvents	[36]
MIP-FI-CL	1.4×10^{-6} -1.6×10^{-4} M	9.3×10^{-7} M	High sensitivity and selectivity; Time-consuming; Detection in drugs samples in aqueous solution	[38]
IDLLME-HPLC-UV	0.5 $-1,000$ ng mL ⁻¹	0.26 ng mL ⁻¹	High specificity, sensitivity and simplicity; Detection in organic solvents	[37]
TLC-HPLC	0.01–0.12 μg	–	Simple, accurate and specific; Detection in organic solvents	[39]
MIP-fluorescence method	0.02 -0.80 mg L ⁻¹	5 μg L ⁻¹	High sensitivity and selectivity; Time-consuming, low cost; Detection in urine and onion skin samples in organic solvents	[40]
LC-ESI-MS/MS	3.28 -328.0 ng mL ⁻¹	0.76 ng mL ⁻¹	Selective, rapid, sensitive; Higher cost; Detection in organic solvents	[41]
Quantum dots-fluorescence	2.65×10^{-6} -7.5×10^{-6} M	5.71×10^{-7} M	Use organic solvent to prepare, high cost, toxic; Detection in aqueous solution	[42]
Fluorescence of carbon nanoparticles	3.3×10^{-6} -41.2×10^{-6} M	1.75×10^{-7} M	Easy synthesis and low cost; sensitive; interferents: other flavones; Detection in aqueous solution	This method

Calibration curves and sensitivity of the method

Figure 4 shows a gradual decrease in PL intensity of the CNPs at 438 nm with an increase of quercetin concentration in fetal bovine serum solution. The binding of quercetin to the CNPs changes the surface of the particles and facilitates nonradiative CNPs/quercetin combination annihilation which induced the quenching of CNPs fluorescence [33]. The PL quenching data followed the Stern–Volmer equation, via a static mechanism [34]:

$$F_0/F = 1 + K_{SV}[S]$$

F and F_0 are the fluorescent intensities of the CNPs in the presence and absence of quercetin in fetal bovine serum solution respectively. $[S]$ is the concentration of quercetin, and K_{SV} is the quenching constant of the quencher.

The calibration for quercetin was constructed from the results obtained under the optimal conditions. The equation, limit of detection and precision were calculated according to the general procedure. The linear regression equation was as follows:

$$F_0/F = 1 + 4.34 \times 10^4[S]$$

The good linear relationship of the values of (F_0/F) with the concentration of quercetin was observed ranging from 3.30 to 41.23×10^{-6} mol L⁻¹ with a correlation coefficient of 0.9931. Quenching constant of the quencher K_{SV} was found to be 4.34×10^4 L mol⁻¹. The detection limit ($S/N = 3$) was found to be 1.75×10^{-7} mol L⁻¹.

Precision and accuracy

To assess the precision and accuracy of this method, determinations were carried out for a set of 10 measurements of $8.27 \times$

10^{-6} , 2.15×10^{-5} and 2.81×10^{-5} mol L⁻¹ quercetin in fetal bovine serum solution under optimal condition respectively. Table S3 (ESM) shows that the quantification results of quercetin were in good agreement with the declared values, and the RSD were 2.8 %, 2.7 % and 2.3 %. These values indicated that this method was accurate and precise. Table 1 summarizes the detection limit, linear range and comments using different methods for the determination of quercetin. Our method was comparable with voltammetric determination [35], electrophoresis with electrochemical detection [36], chemiluminescence sensor [38] and Quantum dots-fluorescence [42]. The results demonstrated that this method offers an easy and sensitive approach for the detection of quercetin in aqueous solution.

Conclusion

In summary, fluorescent CNPs were prepared by self-promoted and self-controlled method without any external heat. Therefore, the carbonization reaction was an automatic synthesis of CNPs. The obtained dark brown mixture was centrifuged and dialyzed to remove ions and residual glucose. Finally, a clear yellow–brown aqueous solution containing CNPs was obtained. The synthesized CNPs showed some benign properties such as strong fluorescence, monodispersity and excellent stability, their luminescence intensity was also stable within the physiological and pathological ranges for ionic strength or pH. The strong fluorescence and excellent water dispersion can be attributed to the abundant surface traps and functional groups. Such CNPs had been further used as a novel sensing probe for label-free, sensitive detection with a low detection limit. Under the optimum conditions, a good linear relationship between fluorescence intensity of the

CNPs and concentration of quercetin in fetal bovine serum solution was observed in wide linear response range. This sensing system had been successfully used for the analysis of quercetin in fetal bovine serum solution. Combining their low cytotoxicity, low cost, stability, convenient and large-scale synthesis, CNPs could provide promising applications in biological labeling and analysis in aqueous media.

Acknowledgments This work was supported by Graduate Students Innovative Projects of Jiangsu Province (No. CXZZ12_0308). We thank the editors and co-workers for help and constructive suggestions.

References

- Häkkinen SH, Kärenlampi SO, Heinonen IM, Mykkänen HM, Törrönen AR (1999) Content of the flavonols quercetin, myricetin, and kaempferol in 25 edible berries. *J Agric Food Chem* 47:2274–2279
- Williamson G, Manach C (2005) Bioavailability and bioefficacy of polyphenols in humans. II. Review of 93 intervention studies. *Am J Clin Nutr* 81:243S–255S
- Loke WM, Proudfoot JM, Stewart S, McKinley AJ, Needs PW, Kroon PA, Hodgson JM, Croft KD (2008) Metabolic transformation has a profound effect on anti-inflammatory activity of flavonoids such as quercetin: lack of association between antioxidant and lipoxygenase inhibitory activity. *Biochem Pharmacol* 75:1045–1053
- Kamaraj S, Vinodhkumar R, Anandakumar P, Jagan S, Ramakrishnan G, Devaki T (2007) The effects of quercetin on antioxidant status and tumor markers in the lung and serum of mice treated with benzo(a)pyrene. *Biol Pharm Bull* 30:2268–2273
- Heijnen CGM, Haenen G, Acker FAA, Vijgh WJF, Bast A (2001) Flavonoids as peroxynitrite scavengers: the role of the hydroxyl groups. *Toxicol in Vitro* 15:3–6
- Alonso-Salces RM, Ndjoko K, Queiroz E, Ioset J, Hostettmann K, Berrueta L, Gallo B, Vicente F (2004) On-line characterisation of apple polyphenols by liquid chromatography coupled with mass spectrometry and ultraviolet absorbance detection. *J Chromatogr A* 1046:89–100
- Sun Y, Guo T, Sui Y, Li F (2003) Quantitative determination of rutin, quercetin, and adenosine in *Flos Carthami* by capillary electrophoresis. *J Sep Sci* 26:1203–1206
- Xiao P, Zhao F, Zeng B (2007) Voltammetric determination of quercetin at a multi-walled carbon nanotubes paste electrode. *Microchem J* 85:244–249
- Sengupta B, Sengupta PK (2002) The interaction of quercetin with human serum albumin: a fluorescence spectroscopic study. *Biochem Biophys Res Commun* 299:400–403
- Mishra B, Barik A, Priyadarsini KI, Mohan H (2005) Fluorescence spectroscopic studies on binding of a flavonoid antioxidant quercetin to serum albumins. *J Chem Sci* 117:641–647
- Baker SN, Baker GA (2010) Luminescent carbon nanodots: emergent nanolights. *Angew Chem Int Ed* 49:6726–6744
- Liu H, Ye T, Mao C (2007) Fluorescent carbon nanoparticles derived from candle soot. *Angew Chem Int Ed* 46:6473–6475
- Bourlino AB, Stassinopoulos A, Anglos D, Zboril R, Karakassides M, Giannelis E (2008) Surface functionalized carbogenic quantum dots. *Small* 4:455–458
- Zhou JG, Booker C, Li R, Zhou XT, Sham TK, Sun XL, Ding ZF (2007) An electrochemical avenue to blue luminescent nanocrystals from multiwalled carbon nanotubes (MWCNTs). *J Am Chem Soc* 129:744–745
- Wang XH, Qu KG, Xu BL, Ren JS, Qu XG (2011) Microwave assisted one-step green synthesis of cell-permeable multicolor photoluminescent carbon dots without surface passivation reagents. *J Mater Chem* 21:2445–2450
- Zong J, Zhu YH, Yang XL, Shen JH, Li CZ (2011) Synthesis of photoluminescent carbogenic dots using mesoporous silica spheres as nanoreactors. *Chem Commun* 47:764–766
- Hu SL, Niu KY, Sun J, Yang J, Zhao NQ, Du XW (2009) One-step synthesis of fluorescent carbon nanoparticles by laser irradiation. *J Mater Chem* 19:484–488
- Wang Q, Liu X, Zhang L, Lv Y (2012) Microwave-assisted synthesis of carbon nanodots through an eggshell membrane and their fluorescent application. *Analyst* 137:5392–5397
- Xiao DL, Yuan DH, He H, Gao MM (2013) Microwave assisted one-step green synthesis of fluorescent carbon nanoparticles from ionic liquids and their application as novel fluorescence probe for quercetin determination. *J Lumin* 140:120–125
- Lu WB, Qin XY, Liu S, Chang GH, Zhang YW, Luo YL, Asiri AM, Al-Youbi AO, Sun XP (2012) Economical, green synthesis of fluorescent carbon nanoparticles and their use as probes for sensitive and selective detection of mercury(II) ions. *Anal Chem* 84:5351–5357
- Dong YQ, Wang RX, Li GL, Chen CQ, Chi YW, Chen GN (2012) Polyamine-functionalized carbon quantum dots as fluorescent probes for selective and sensitive detection of copper ions. *Anal Chem* 84:6220–6224
- Li H, Zhang Y, Wang L, Tian J, Sun X (2011) Nucleic acid detection using carbon nanoparticles as a fluorescent sensing platform. *Chem Commun* 47:961–963
- Fang YX, Guo SJ, Li D, Zhu CZ, Ren W, Dong SJ, Wang EK (2012) Easy synthesis and imaging applications of cross-linked green fluorescent hollow carbon nanoparticles. *ACS Nano* 6:400–409
- Zhang JC, Shen WQ, Pan DY, Zhang ZW, Fang YG, Wu MH (2010) Controlled synthesis of green and blue luminescent carbon nanoparticles with high yields by the carbonization of sucrose. *New J Chem* 34:591–593
- Van Wazer JR (1958) Phosphorus and its compounds. Interscience, New York
- Eda G, Lin YY, Mattevi C, Yamaguchi H, Chen H, Chen I, Chen CW, Chhowalla M (2010) Blue photoluminescence from chemically derived graphene oxide. *Adv Mater* 22:505–509
- Bose R, McMillan JF, Gao J, Rickey KM, Chen CJ, Talapin DV, Murray CB, Wong CW (2008) Temperature-tuning of near-infrared monodisperse quantum dot solids at 1.5 μm for controllable Förster energy transfer. *Nano Lett* 8:2006–2011
- Lunz M, Bradley AL, Chen WY, Gerard VA, Byrne SJ, Gun'ko YK, Lesnyak V, Gaponik N (2010) Influence of quantum dot concentration on Förster resonant energy transfer in monodispersed nanocrystal quantum dot monolayers. *Phys Rev B* 81:201356
- Zhu H, Wang X, Li Y, Wang Z, Yang F, Yang X (2009) Microwave synthesis of fluorescent carbon nanoparticles with electrochemiluminescence properties. *Chem Commun* 5118–5120
- Zhang B, Liu C, Liu Y (2010) A novel one-step approach to synthesize fluorescent carbon nanoparticles. *Eur J Inorg Chem* 4411–4414
- Jin WJ, Costa-Fernández JM, Pereiro R, Sanz-Medel A (2004) Surface-modified CdSe quantum dots as luminescent probes for cyanide determination. *Anal Chim Acta* 522:1–8
- Nazzal AY, Qu LH, Peng XG, Xiao M (2003) Photoactivated CdSe nanocrystals as nanosensors for gases. *Nano Lett* 3:819–822
- Liu M, Xu L, Cheng W, Zeng Y, Yan Z (2008) Surface-modified CdS quantum dots as luminescent probes for sulfadiazine determination. *Spectrochim Acta A Mol Biomol Spectrosc* 70:1198–1202
- Long Y, Jiang D, Zhu X, Wang J, Zhou F (2009) Trace Hg^{2+} analysis via quenching of the fluorescence of a CdS-encapsulated DNA nanocomposite. *Anal Chem* 81:2652–2657

35. He JB, Lin XQ, Pan J (2005) Multi-wall carbon nanotube paste electrode for adsorptive stripping determination of quercetin: a comparison with graphite paste electrode via voltammetry and chronopotentiometry. *Electroanalysis* 17:1681–1686
36. Chen G, Zhang H, Ye J (2000) Determination of rutin and quercetin in plants by capillary electrophoresis with electrochemical detection. *Anal Chim Acta* 423:69–76
37. Ranjbari E, Biparva P, Hadjmohammadi MR (2012) Utilization of inverted dispersive liquid–liquid microextraction followed by HPLC-UV as a sensitive and efficient method for the extraction and determination of quercetin in honey and biological samples. *Talanta* 89:117–123
38. Qiu H, Luo C, Sun M, Lu F, Fan L, Li X (2012) A novel chemiluminescence sensor for determination of quercetin based on molecularly imprinted polymeric microspheres. *Food Chem* 134:469–473
39. Shao J, Guo M, Fan Q, Cheng F (2011) Study on quality control methods for different varieties of *Meconopsis* of Gansu. *Zhong Yao Cai* 34:1678–1681
40. Hu Y, Feng T, Li G (2014) A novel solid fluorescence method for the fast determination of quercetin in biological samples based on the quercetin-Al(III) complex imprinted polymer. *Spectrochim Acta A Mol Biomol Spectrosc* 118:921–928
41. Chang L, Zhang XX, Ren YP, Cao L, Zhi XR, Zhang LT (2013) Simultaneous quantification of six major flavonoids from *Fructus sophorae* by LC-ESI-MS/MS and statistical analysis. *Indian J Pharm Sci* 75:330–338
42. Wu D, Chen Z (2013) ZnS quantum dots-based fluorescence spectroscopic technique for the detection of quercetin. *Luminescence*. doi:10.1002/bio.2545